Available online at www.sciencedirect.com
ScienceDirect
International Journal of Mass Spectrometry 268 (2007) 38–46
International Journal of Mass Spectrometry
www.elsevier.com/locate/ijms

# GeoVOC: A SIFT-MS method for the analysis of small linear hydrocarbons of relevance to oil exploration

Gregory J. Francis [a,b], Paul F. Wilson [a,b], Daniel B. Milligan [a,b], Vaughan S. Langford [a,b], Murray J. McEwan [a,b,*]

[a] *Department of Chemistry, University of Canterbury, Christchurch 8041, New Zealand*
[b] *Syft Technologies, Middleton, Christchurch 8024, New Zealand*

Received 2 July 2007; received in revised form 10 August 2007; accepted 11 August 2007
Available online 19 August 2007

**Abstract**

The rate coefficients of the ion–molecule reactions between $O_2^{\bullet+}$, $H_3O^+$, and a range of linear saturated hydrocarbons, and between common hydrocarbon product ions from these reactions and water were determined using a flowing afterglow selected ion flow tube mass spectrometer. Using these data, the selected ion flow tube-mass spectrometry (SIFT-MS) technique was applied to the real-time measurement of linear saturated hydrocarbons in dry and moist headspace samples without sample preparation. Using a Voice100 SIFT-MS instrument the Geochemical VOC method (GeoVOC) has been assessed against calibrated standards and found to give an experimental RMS precision to within 2% for dry and 6% for humid hydrocarbon samples in the ppm range. The application of SIFT-MS and development of the GeoVOC method offers a fast convenient means of assessment of hydrocarbon seeps.


*Keywords:* Selected ion flow tube; Hydrocarbon; Ion–molecule; Oil prospecting

## 1. Introduction

Near-surface hydrocarbon analysis (the detection and analysis of light hydrocarbon micro-seeps) has traditionally played an important role in explorations of new petroleum fields [1]. In the past this analysis has primarily relied on the use of microwave emission or GC-based detection techniques [2,3]. However, both of these detection methods have significant drawbacks. Microwave spectroscopy is highly unspecific and can often lead to false positives [4], and as with most GC-based techniques, long column elution times lead to this being a very time consuming and therefore expensive method for analysis.

In comparison to microwave and GC-based analyses, selected ion flow tube-mass spectrometry (SIFT-MS) is a technique which can specifically analyse and quantify headspace gas in real time [5–7]. Analyte specificity is enabled by using three chemical ionisation precursors for analysis ($H_3O^+$, $NO^+$ and $O_2^{\bullet+}$). Because SIFT-MS does not involve column-based separation, sample throughput is rapid (approximately 60 samples per hour) and therefore is a much more cost effective technique. However, knowledge of the chemical kinetics (rate coefficients and branching ratios) of each individual analyte's reaction with a precursor ion is required.

For acyclic hydrocarbon analysis, $O_2^{\bullet+}$ is the precursor ion of choice as its ionisation energy is large enough to give electron transfer to the smaller hydrocarbons. A previous investigation by this group [8] used helium as a carrier gas and studied a range of $C_1$–$C_4$ hydrocarbons. With hydrocarbons containing more than four carbon atoms, the reactions with $H_3O^+$ need to be appraised as well as the pseudo-bimolecular rate coefficients for $H_3O^+$ clustering with the hydrocarbon analyte when it becomes fast enough to be measurable [9,10].

'Geochemical volatile organic compound analysis' (GeoVOC) is a method for analysing small volatile hydrocarbons present in oil and gas seeps. However, the 'GeoVOC' method of analysis using SIFT-MS has been hindered by two important factors. First, the kinetic parameters for the alkanes have been studied on few occasions with the reagent ions used in SIFT-MS. Second, the reaction chemistry of the

* Corresponding author at: Department of Chemistry, University of Canterbury, Christchurch 8041, New Zealand. Tel.: +64 3 364 2875; fax: +64 3 364 2110.
*E-mail address:* murray.mcewan@canterbury.ac.nz (M.J. McEwan).

1387-3806/$ – see front matter © 2007 Elsevier B.V. All rights reserved.
doi:10.1016/j.ijms.2007.08.005

product ions formed in these reactions with water has not been well-studied. A thorough understanding of the chemistry of SIFT-MS product ions reacting with water is important due to the high concentrations of water often present in the reaction region of the flow tube. This article resolves both these issues in that the reagent ion chemistry has been extended to cover $C_1$–$C_9$ alkanes, and the secondary reactions of the product ions of the $C_1$–$C_8$ alkanes with $H_2O$ have been investigated. A rapid, non-selective, in-line sample drying system has then been employed for quantitation of hydrocarbons across a range of moist soil samples, and even bore water samples.

## 2. Experimental

### 2.1. Kinetic data collection using FA-SIFT

Two selected ion flow tube instruments were used in this study. The FA-SIFT instrument at the University of Canterbury (UoC FA-SIFT) has been described previously [11]. The reactions described in this work were carried out using a reaction flow tube length of 50 cm, a tube diameter of 7.3 cm, and a total flow tube pressure of 0.25 Torr of helium and argon carrier gas at 298 K. The carrier gases are allowed into the flow tube via two concentric annuli; the inner injecting helium at 40% and the outer injecting argon at 60% of the total flow. Helium is used on the inner orifice to create the venturi effect, and thermalise ions entering the flow tube, while argon is added to the flow tube to decrease the zero field mobility of ions in a carrier gas [12].

The $O_2^{\bullet+}$ and $H_3O^+$ ions were generated in a flowing afterglow by chemical ionisation from helium, which was in turn generated in a microwave discharge. The ions formed in the afterglow were sampled through a 2 mm orifice into a low-pressure region where they were mass selected by the upstream quadrupole mass filter. These mass selected ions were introduced into the SIFT flow tube via the venturi orifice. Rate coefficients and branching ratios were measured in the usual way by observing the semi-logarithmic decay of the ion signal with reactant gas flow [13]. Rate coefficients have an error of ±20%.

Reactions of hydrocarbon ions with $H_2O$ were performed where possible, by creating the hydrocarbon ion in the flowing afterglow and injecting it after mass selection into the flow tube, or, if the ion was found to break up on injection, creating the ion in the flow tube by chemical ionisation from $O_2^{\bullet+}$. The hydrocarbon ions were then reacted with $H_2O$/He mixtures of known composition. $H_2O$/He composition ratios were determined by the well-understood reaction of $Ar^+$ with $H_2O$ [14]. We estimate that the rate coefficients measured using $H_2O$/He mixtures have an uncertainty of ±30% based on the inherent uncertainties of measuring rate coefficients, and the accuracy of the $H_2O$/He mixtures.

Collision limiting rate coefficients are determined using the method of Su and Chesnavich [15]. Literature values of the polarizabilities and the dipole moment of $H_2O$ were taken from the CRC Handbook of Chemistry and Physics [16].

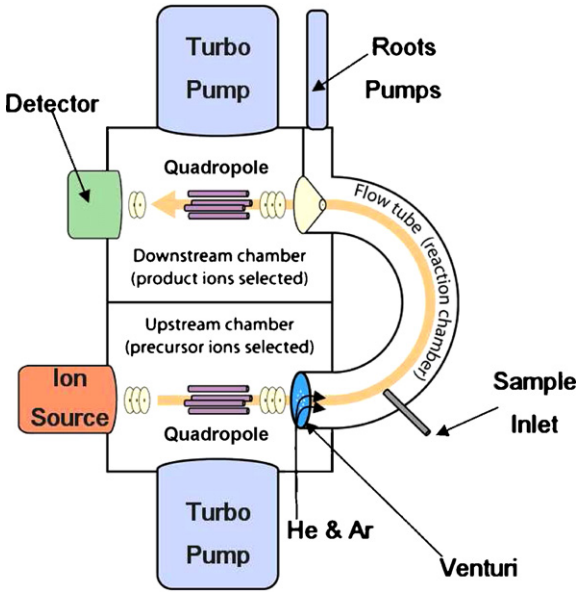


Fig. 1. A schematic diagram of the Voice100 SIFT-MS instrument.

### 2.2. Hydrocarbon quantitation using voice100 SIFT-MS

The instrument used for the quantitative measurement of hydrocarbons in moist soil samples, bore water samples and gas phase bore samples is a commercial Voice100 SIFT-MS instrument (Syft Technologies, Christchurch, New Zealand), which has been described previously [17–19], and shall only be discussed briefly here.

In the Voice100, shown in Fig. 1, ions are generated by a microwave discharge acting on and ionising a saturated air/water mixture at ~0.3 Torr. Reagent ions ($H_3O^+$, $NO^+$ and $O_2^{\bullet+}$) are individually mass selected in the upstream chamber (at $\sim 1 \times 10^{-5}$ Torr) by a quadrupole mass filter, and injected against the pressure gradient into the flow tube through a venturi orifice.

Hydrocarbon headspace samples are introduced into the flow tube at approximately 220 ml atmosphere $min^{-1}$ at a distance of 6 cm from the venturi. Ion/molecule reactions are carried out in the reaction region, which is approximately 25 cm long, with a measured ion transit time of 4 ms. Ions are then sampled through an electrostatic orifice at the end of the flow tube, into the downstream chamber. On entering the downstream chamber (at $<1 \times 10^{-5}$ Torr), ions resulting from the ion/molecule reaction of interest are mass selected by a second quadrupole mass spectrometer, and detected on a continuous dynode particle multiplier.

The flow tube is approximately 30 cm long and 5 cm in diameter and is bent through 180°, so as to stack the downstream on the upstream chamber, and therefore minimise the overall footprint of the instrument. Both the upstream and the downstream chambers are pumped by 500 l $s^{-1}$ turbo-molecular pumps, and flow tube gases are removed by a roots blower (100 l $s^{-1}$ at 0.5 Torr). The venturi orifice used on a Voice100 is a dual inlet system, where helium is used to create the venturi effect on an inner annulus, and argon is added through a second annulus on

the venturi plate which is further from the centre. All experiments were performed with a flow tube pressure of 0.5 Torr, and a carrier gas mixture of 40% helium to 60% argon.

As mass discrimination functions of both the UoC FA-SIFT and the Voice100 are known and well understood, such that a product ion branching ratio measured on one instrument is easily transported to another.

Hydrocarbon headspace samples are introduced into the Voice100 flow tube through Nafion$^{TM}$ tubing (Perma Pure LLC, Toms River, NJ, USA) encased in a rapid purge flow of nitrogen. Nafion$^{TM}$ tubing is a co-polymer of teflon and perfluoro-3,6-dioxa-4-methyl-7-octene-sulfonic acid, which is unreactive to non-polar compounds such as hydrocarbons, but reactively diffuses polar water molecules across a concentration gradient. By flowing dry nitrogen over the outer surface of the Nafion$^{TM}$ tubing, water molecules diffuse across the concentration gradient from the moist sample into the nitrogen purge flow, while leaving hydrocarbon concentrations unaltered [20].

### 2.3. Chemicals

Linear $C_1$–$C_9$ hydrocarbon compounds were obtained from Sigma–Aldrich (Sydney, Australia), and were purified by freeze-pump-thaw cycling. Hydrocarbon standards for validation of the GeoVOC method were obtained from Scott Specialty Gases (Plumsteadville, PA, USA) and BOC Gases (Auckland, New Zealand). To simulate the moist headspace of a soil or water sample, tedlar bags were partially filled with the hydrocarbon standards and 1 ml of water, then left to equilibrate for 1 h at 20 °C.

### 2.4. Current GeoVOC analysis method

Two separate sample types can be presented to a SIFT-MS for GeoVOC analysis; these are soil samples, and water samples. The soil technique ($GeoVOC_s$) involves sampling 150–500 g of soil into a robust canister from at least 2 m below the surface (to ensure minimisation of any aerobic microbial activity). Upon their arrival at the laboratory, the samples are incubated at 20 °C overnight. The lid of each can is then pierced with a punch and the headspace above the soil samples is introduced into the SIFT-MS for analysis through the Nafion$^{TM}$ dryer. Soil samples can also be taken from various depths as a well is being drilled; the same processing applies to these samples.

The water technique ($GeoVOC_w$) involves sampling 100–500 ml of bore water (from drinking or irrigation water wells), which generally arises from at least 50 m below the surface, into disposable mineral water bottles (~750 ml). The bore water is sampled in a controlled fashion so as to not dilute the hydrocarbons in the sample. As the Henry's law constant of small hydrocarbons in water lies substantially toward the small hydrocarbons being in the gas phase [21], almost all hydrocarbons dissolved in the bore water at high pressures below the surface will move into the gas phase once inside the sampling vessel. The headspace is then introduced into the SIFT-MS (via the Nafion$^{TM}$ dryer) by piercing the bottle using a sampling needle.

Similar analysis can also be applied to neat gas samples taken directly from an oil/gas well. Due to the high concentrations of hydrocarbons often found in these types of samples, the sample flow rate into the Voice100 is reduced to ensure precursor signals are not substantially reduced.

By observing the empirical composition ratios of small linear and branched hydrocarbons above oil and gas reservoirs, a reservoir type can be determined [3].

## 3. Results and discussion

The reactions that have been investigated in this work are summarized in Table 1($O_2^{\bullet+} + n$-$C_xH_y$), Table 2 ($H_3O^+ + n$-$C_xH_y$) and Table 3 ($C_xH_y^+ + H_2O$).

A previous investigation of similar nature [8] had difficulty generating $O_2^{\bullet+}$ completely free of the $O_2^{+}$* species. Formation of the excited ion was postulated to be via Penning ionisation of metastable helium atoms in the flowing afterglow to give $O_2^+$ ($a^4\Pi_u$). This ion will exist in the flow tube, when using a helium carrier gas, because collisional quenching via helium is an inefficient process [35]. In previous studies by Ferguson and co-workers [36–38], Penning ionisation was observed by studying the reaction of $O_2^+$ with methane and detecting product ions other than $CH_2OOH^+$ (*m*/*z* 47). However, in the study presented here, no product ions other than *m*/*z* 47 were observed for the $O_2^{\bullet+}$ + methane reaction and therefore if the Penning ionised $O_2^+$ ($a^4\Pi_u$) was forming, the ion was short-lived. The lack of $O_2^+$ ($a^4\Pi_u$) is attributed to the addition of argon to the flow tube. Argon is in excess compared to the standard carrier gas helium, which will facilitate effective relaxation of the excited $O_2^+$ ($a^4\Pi_u$) to the ground state $O_2^+$ ($x^4\Pi_u$) as collisional quenching of $O_2^+$ ($a^4\Pi_u$) by argon is an efficient process [35]. Therefore, in the Voice100, any $O_2^+$ ($a^4\Pi_u$) formed from the microwave discharge will also be quickly relaxed to $O_2^+$ ($x^4\Pi_u$) by collisions with argon atoms and will not affect the chemistry observed here.

Calculation of enthalpies of reaction assume that the barrier for isomerisation of ions will always be less than the product ion's internal energy, and therefore an ion will exist in its lowest energy structural isomer, i.e., $C_4H_9^+$ will always exist as the *tert*-butyl cation. However, due to the nature of SIFT-MS, we are unable to characterise the neutral products, therefore any neutral structures claimed are tentative. The enthalpy of formation of $n$-$C_9H_{20}$ was determined from a linear extrapolation of smaller linear hydrocarbons. Proton affinities are given in Tables 2 and 3 where available. The proton affinity of $C_5H_{10}$ is an estimate based on a similar structure. All thermodynamic data for this work were obtained from the NIST webbook database [39].

### 3.1. Reactions of $O_2^{\bullet+}$ + n-$C_xH_y$

Reactions of methane, ethane, propane and butane with $O_2^{\bullet+}$ in the UoC FA-SIFT-MS have been published by this group [8], and repetition of these reactions is only to illustrate the similarity between bimolecular reactions occurring in differing carrier gas compositions. The differences between the current and previous measurements are within experimental error (±20%). The mea-

Table 1
Reactions of $O_2^{\bullet+}$ with the given hydrocarbon measured at 298 K, 0.25 Torr, with a carrier gas mixture of 40% helium, 60% argon

| Neutral molecule | IE (eV)[a] | Products | Branching ratio | Rate coefficient[b,c] | Previous measurements |
|---|---|---|---|---|---|
| $CH_4$ | 12.61 | $CH_2OOH^+ + H$ | 1.00 | 0.006(1.2) | 0.005[d,e], 0.052,[f] 0.063[g] |
| $C_2H_6$ | 11.52 | $C_2H_6^+ + O_2$ | 0.30 | 0.97(1.3) | 1.1[d], 1.2[h] |
| | | $C_2H_5^+ + (O_2 + H)$ | 0.55 | | |
| | | $C_2H_4^+ + O_2 + H_2$ | 0.15 | | |
| $C_3H_8$ | 10.94 | $C_3H_8^+ + O_2$ | 0.15 | 1.2(1.4) | 1.4[d,h] |
| | | $C_3H_7^+ + (O_2 + H)$ | 0.40 | | |
| | | $C_3H_6^+ + O_2 + H_2$ | 0.05 | | |
| | | $C_2H_5^+ + O_2 + (CH_3)$ | 0.05 | | |
| | | $C_2H_4^+ + O_2 + (CH_4)$ | 0.35 | | |
| $C_4H_{10}$ | 10.57 | $C_4H_{10}^+ + O_2$ | 0.25 | 1.4(1.5) | 1.4[d], 2.0[h], 1.5[i] |
| | | $C_4H_9^+ + (O_2 + H)$ | 0.05 | | |
| | | $C_3H_7^+ + O_2 + (CH_3)$ | 0.60 | | |
| | | $C_3H_6^+ + O_2 + (CH_4)$ | 0.05 | | |
| | | $C_2H_4^+ + O_2 + (C_2H_6)$ | 0.05 | | |
| $C_5H_{12}$ | 10.28 | $C_5H_{12}^+ + O_2$ | 0.20 | 1.5(1.6) | 1.6[i], 0.8[j] |
| | | $C_4H_9^+ + O_2 + (CH_3)$ | 0.10 | | |
| | | $C_3H_7^+ + O_2 + (C_2H_5)$ | 0.30 | | |
| | | $C_3H_6^+ + O_2 + (C_2H_6)$ | 0.40 | | |
| $C_6H_{14}$ | 10.13 | $C_6H_{14}^+ + O_2$ | 0.20 | 1.8(1.7) | 1.99[h], 1.7[i] |
| | | $C_5H_{11}^+ + O_2 + (CH_3)$ | 0.05 | | |
| | | $C_4H_9^+ + O_2 + (C_2H_5)$ | 0.35 | | |
| | | $C_4H_8^+ + O_2 + (C_2H_6)$ | 0.25 | | |
| | | $C_3H_7^+ + O_2 + (C_3H_7)$ | 0.05 | | |
| | | $C_3H_6^+ + O_2 + (C_3H_8)$ | 0.10 | | |
| $C_7H_{16}$ | 9.93 | $C_7H_{16}^+ + O_2$ | 0.15 | 1.7(1.8) | |
| | | $C_5H_{11}^+ + O_2 + (C_2H_5)$ | 0.30 | | |
| | | $C_5H_{10}^+ + O_2 + (C_2H_6)$ | 0.15 | | |
| | | $C_4H_9^+ + O_2 + (C_3H_7)$ | 0.15 | | |
| | | $C_4H_8^+ + O_2 + (C_3H_8)$ | 0.15 | | |
| | | $C_3H_7^+ + O_2 + (C_4H_9)$ | 0.05 | | |
| | | $C_3H_6^+ + O_2 + (C_4H_{10})$ | 0.05 | | |
| $C_8H_{18}$ | 9.80 | $C_8H_{18}^+ + O_2$ | 0.15 | 1.9(1.9) | 1.8[k] |
| | | $C_6H_{13}^+ + O_2 + (C_2H_5)$ | 0.30 | | |
| | | $C_6H_{12}^+ + O_2 + (C_2H_6)$ | 0.10 | | |
| | | $C_5H_{11}^+ + O_2 + (C_3H_7)$ | 0.15 | | |
| | | $C_5H_{10}^+ + O_2 + (C_3H_8)$ | 0.10 | | |
| | | $C_4H_9^+ + O_2 + (C_4H_9)$ | 0.10 | | |
| | | $C_4H_8^+ + O_2 + (C_4H_{10})$ | 0.10 | | |
| $C_9H_{20}$ | 9.71 | $C_9H_{20}^+ + O_2$ | 0.05 | 2.1 (2.0) | |
| | | $C_7H_{15}^+ + O_2 + (C_2H_5)$ | 0.10 | | |
| | | $C_7H_{14}^+ + O_2 + (C_2H_6)$ | 0.05 | | |
| | | $C_6H_{13}^+ + O_2 + (C_3H_7)$ | 0.20 | | |
| | | $C_6H_{12}^+ + O_2 + (C_3H_8)$ | 0.05 | | |
| | | $C_5H_{11}^+ + O_2 + (C_4H_9)$ | 0.10 | | |
| | | $C_5H_{10}^+ + O_2 + (C_4H_{10})$ | 0.10 | | |
| | | $C_4H_9^+ + O_2 + (C_5H_{11})$ | 0.25 | | |
| | | $C_4H_8^+ + O_2 + (C_5H_{12})$ | 0.10 | | |

[a] Ionisation energies are sourced from the NIST webbook database [22].
[b] The rate coefficient is listed in units of $10^{-9}$ cm$^3$ molecule$^{-1}$ s$^{-1}$.
[c] The calculated collision rate (in units of $10^{-9}$ cm$^3$ molecule$^{-1}$ s$^{-1}$) is shown in parenthesis.
[d] Ref. [8].
[e] Ref. [23].
[f] Ref [24].
[g] Ref. [25].
[h] Ref. [26].
[i] Ref. [10].
[j] Ref. [27].
[k] Ref. [28].

Table 2
Reactions of $H_3O^+$ with the given hydrocarbon measured at 298 K, 0.25 Torr with a carrier gas mixture of 40% helium and 60% argon

| Neutral molecule | PA (kJ mol$^{-1}$)[a] | Products | Branching ratio | Rate coefficient[b,c] | Previous measurements |
|---|---|---|---|---|---|
| $CH_4$ | 543.5 | No reaction | | | No reaction[d] |
| $C_2H_6$ | 596.3 | No reaction | | | No reaction[d] |
| $C_3H_8$ | 625.7 | No reaction | | | No reaction[d,e] |
| $C_4H_{10}$ | | No reaction | | | 0.003[d,e], n.r.[f] |
| $C_5H_{12}$ | | Adduct | 1.00 | 0.15 (1.9) | |
| $C_6H_{14}$ | | Adduct | 1.00 | 0.19 (2.0) | <0.1[f], 0.03[g] |
| $C_7H_{16}$ | | Adduct | 1.00 | 0.40 (2.2) | 0.26[g] |
| $C_8H_{18}$ | | Adduct | 1.00 | 0.50 (2.3) | 0.9[f], 0.58[g] |

[a] Proton affinities are sourced from the NIST webbook database [22].
[b] The rate coefficient is listed in units of $10^{-9}$ cm$^3$ molecule$^{-1}$ s$^{-1}$.
[c] The calculated collision rate (in units of $10^{-9}$ cm$^3$ molecule$^{-1}$ s$^{-1}$) is shown in parenthesis.
[d] Ref. [8].
[e] Ref. [29].
[f] Ref. [10].
[g] Ref. [30].

sured rate for $O_2^{\bullet+} + CH_4$ is observed to be 20% faster than the previous measurement on this instrument, which is attributed to the presence of argon in the flow tube, as the reaction is known to be termolecular, and therefore dependant on carrier gas [36].

New minor exothermic product channels have been observed for the reaction of $O_2^{\bullet+}$ + propane and butane, however these may be due to impurities in the analyte sample.

The reactions of the larger hydrocarbons, which have not been previously measured on the UoC FA-SIFT are observed with rapid electron transfer and dissociative electron transfer being the major product channels.

Pentane is observed to react in a similar fashion to the previous study by Smith and Spanel [10]. A small product channel attributed to $C_4H_8^+$ (<5%) was also observed, however difficulty arose in determining whether this ion was primary, secondary or due to an impurity. Formation of $C_4H_8^+$ is postulated to be a very exothermic process (shown as Eq. (1)) and the observation of this ion is attributed to the addition of argon to

Table 3
Reactions of the given ion with $H_2O$ measured at 298 K, 0.5 Torr with a carrier gas mixture of 40% helium and 60% argon

| Ion | PA (conj. base) (kJ mol$^{-1}$)[a] | Products | Branching ratio | Rate coefficient[b,c] | Previous measurements |
|---|---|---|---|---|---|
| $CH_2OOH^+$ | | Adduct | 1.00 | 0.02 (2.5) | 0.021[d] |
| $C_2H_4^+$ | 755.2 | Adduct | 1.00 | 0.025 (2.7) | No reaction[e] |
| $C_2H_5^+$ | 680.5 | $H_3O^+ + C_2H_4$ | 1.00 | 2.5 (2.7) | 1.86[f], 6.0[g] |
| $C_2H_6^+$ | 616 | $H_3O^+ + C_2H_5$ | 1.00 | 2.2 (2.7) | 2.95[g], 1.2[i] |
| $C_3H_6^+$ | 736 | Adduct | 1.00 | 0.05 (2.5) | |
| $C_3H_7^+$ | 751.6 | Adduct | 1.00 | 0.007 (2.5) | |
| $C_3H_8^+$ | 671.4 | $H_3O^+ + C_3H_7$ | 1.00 | 2.3 (2.5) | 1.4[i] |
| $C_4H_8^+$ | 785 | No reaction | | | |
| $C_4H_9^+$ | 802 | No reaction | | | |
| $C_4H_{10}^+$ | | Adduct | 1.00 | 0.04 (2.4) | 0.041–0.044[h] |
| $C_5H_{10}^+$ | | No reaction | | | |
| $C_5H_{11}^+$ | (808) | No reaction | | | |
| $C_5H_{12}^+$ | | Adduct | 1.00 | 0.05 (2.4) | |
| $C_6H_{12}^+$ | | Adduct | 1.00 | 0.004 (2.3) | |
| $C_6H_{13}^+$ | 813.9 | Adduct | 1.00 | 0.004 (2.3) | |
| $C_6H_{14}^+$ | | Adduct | 1.00 | 0.004 (2.3) | 0.0015–0.0056[h] |
| $C_7H_{14}^+$ | | No reaction | | | |
| $C_7H_{16}^+$ | | No reaction | | | |
| $C_8H_{16}^+$ | | No reaction | | | |
| $C_8H_{17}^+$ | | No reaction | | | |
| $C_8H_{18}^+$ | | Adduct | 1.00 | 0.002 (2.3) | |

[a] Proton affinities are sourced from the NIST webbook database [22].
[b] The rate coefficient is listed in units of $10^{-9}$ cm$^3$ molecule$^{-1}$ s$^{-1}$.
[c] The calculated collision rate (in units of $10^{-9}$ cm$^3$ molecule$^{-1}$ s$^{-1}$) is shown in parenthesis.
[d] Ref. [23].
[e] Ref. [31].
[f] Ref. [14].
[g] Ref. [32].
[h] Ref. [33].
[i] Ref. [34].

the carrier gas, leading to faster thermalisation of high energy products.

$$O_2^{\bullet+} + C_5H_{12} \rightarrow C_4H_8^+ + O_2 + CH_4 \quad (< 0.05)$$
$$\Delta H^\circ = -226\,\text{kJ mol}^{-1} \quad (1)$$

Again for hexane, results are similar to previous investigations by Smith and Spanel [10], however in this study individual ion branching ratios are included. The observed rate coefficient for $O_2^{\bullet+}$ reacting with hexane is slightly faster than collision rate, but within the ±20% experimental error.

No previous measurement of the chemistry of heptane or nonane with $O_2^{\bullet+}$ was found in the literature. Both reactions proceeded as expected, with a reaction efficiency approaching unity and with the observation of common product ions.

The commonly observed product ions from the $O_2^{\bullet+} + C_7H_{16}$ and $C_9H_{18}$ reactions at *m/z* 71, *m/z* 57 and *m/z* 43 are assumed to be the thermodynamically stable 2-methylbutyl ($C_5H_{11}^+$ $\Delta H_f^\circ = 661\,\text{kJ mol}^{-1}$), tert-butyl ($C_4H_9^+$ $\Delta H_f^\circ = 693\,\text{kJ mol}^{-1}$), and *iso*-propyl ($C_3H_7^+$ $\Delta H_f^\circ = 798\,\text{kJ mol}^{-1}$) cations, respectively. Because SIFT-MS requires product ions explicitly from a single analyte in order to monitor that analyte, common product ions are hindrances to using SIFT-MS as a detection method for hydrocarbons.

### 3.2. Reactions of $H_3O^+$ + *n*-$C_xH_y$

Table 2 displays bimolecular rate coefficients for the association reactions of $H_3O^+$ with linear hydrocarbons at the given conditions. Even though the proton affinities of only methane, ethane and propane are known, it is assumed that all linear hydrocarbons measured in this study have a proton affinity less than 691 kJ mol$^{-1}$ (the proton affinity of water); above this amount, exothermic proton transfer is expected.

Pseudo-bimolecular rate coefficients were fast enough to be measurable for *n*-$C_5H_{12}$, *n*-$C_6H_{14}$, *n*-$C_7H_{16}$ and *n*-$C_8H_{18}$. However, when $H_3O^+$ was reacted with the smaller hydrocarbons the $H_3O^+$ intensity was observed to increase, probably due to the analyte in the flow tube at the concentrations required for kinetic measurements, altering the diffusion characteristics of the $H_3O^+$ ion.

As noted by Smith and Spanel [10], where an adduct ion was found to form from the reaction of $H_3O^+ + M$, the resulting $H_3O^+$. M was found to rapidly cluster with a second water molecule in the presence of water vapour.

### 3.3. Reactions of *n*-$C_xH_y^+ + H_2O$

Because samples introduced into the SIFT-MS instruments are generally whole air samples, or headspaces above volatile compounds, water is generally the major reactive analyte present (0.5–6%).To be useful for SIFT-MS analysis any ion present that will react with water must form new ions which can be detected explicitly, i.e., not reform $H_3O^+$. When the concentration of water is high, any product ion formed, for which the proton affinity of the conjugate base is less than the proton affinity of water (691 kJ mol$^{-1}$) will not be seen, or will at least be substantially reduced, as it will proton transfer to water in the flow tube.

Ions observed to proton transfer to water are given in Eqs. (2)–(4), and these reactions were observed to occur with a reaction efficiency at or very near unity.

$$C_2H_5^+ + H_2O \rightarrow H_3O^+ + C_2H_4 \quad (1.00)$$
$$\Delta H^\circ = -11\,\text{kJ mol}^{-1} \quad (2)$$

$$C_2H_6^+ + H_2O \rightarrow H_3O^+ + C_2H_5 \quad (1.00)$$
$$\Delta H^\circ = -75\,\text{kJ mol}^{-1} \quad (3)$$

$$C_3H_8^+ + H_2O \rightarrow H_3O^+ + C_3H_7 \quad (1.00)$$
$$\Delta H^\circ = -20\,\text{kJ mol}^{-1} \quad (4)$$

Reactions (2)–(4) are aided by the very thermodynamically stable neutral species which are formed during the reaction and that provide exoergic pathways.

### 3.4. Other important secondary chemistry

Even though water is the major reactive analyte in most SIFT-MS samples, secondary chemistry of other analytes may also play an important role in elucidating the concentrations of hydrocarbons in soil headspace. From the literature it is known that $C_2H_4^+$ will react rapidly with small hydrocarbons to produce $C_3H_7^+$ [40]. This will skew the observed product branching ratios in the favour of $C_3H_7^+$, a product observed from most reactions of $O_2^{\bullet+}$ with the linear hydrocarbons studied. However, because hydrocarbon concentrations are usually in the low to mid parts-per-million by volume (ppmv) concentration range for a standard GeoVOC sample, the number density of analyte in the flow tube is low enough to have minimal effect on the relative ratios of primary product ions. This secondary chemistry is currently not taken into account in the GeoVOC method, as the outcomes are deemed to have an immeasurably small effect (less than 0.5% alteration of product branching ratios).

## 4. GeoVOC validation and examples

Because of the sensitivity of the GeoVOC method to water, humid hydrocarbon-rich headspace samples must be dried to a constant low humidity so as to not alter the observable concentration. Nafion tubing encased in a nitrogen purge flow (as described in the Section 2) has been found to be an effective system for drying whole air samples from completely saturated (∼6% water) to low water concentrations (>0.4%). Fig. 2 shows the effect of a Nafion dryer on the intensity of hydronium ion water clusters observed in a SIFT-MS selected ion monitoring spectrum. The relative intensities of the hydronium ion water clusters detected are indicative of the total water concentration entering the flow tube [41].

### 4.1. GeoVOC method

The concentrations of butane, pentane, hexane, heptane, octane and nonane are determined by measuring the ratio of

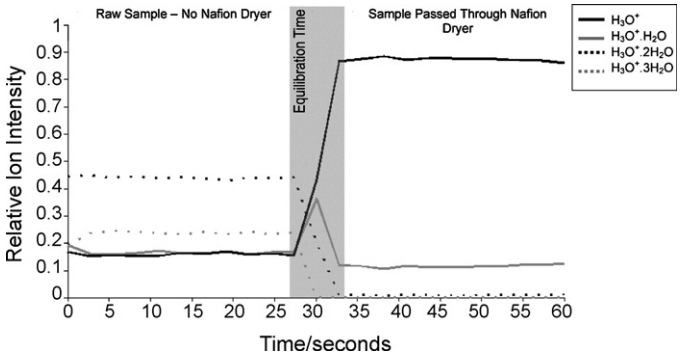


Fig. 2. Drying efficiency of a Nafion dryer system incorporated into a SIFT-MS. Humid air is passed into the SIFT-MS without and with a Nafion dryer, with a short equilibration time between the two.

the molecular product ion ($C_4H_{10}^+$, $C_5H_{12}^+$, $C_6H_{14}^+$, $C_7H_{16}^+$, $C_8H_{18}^+$ and $C_9H_{20}^+$, respectively) divided by its branching ratio with $O_2^{\bullet+}$. Propane can also be determined in a similar way, by the ratio of $C_3H_8^+$ divided by its branching ratio with $O_2^{\bullet+}$. Because the concentration of water entering the flow tube is very low (<0.4%) the $C_3H_8^+$ concentration is not substantially perturbed by reactions with $H_2O$. Ethane concentrations are measured by monitoring the ratio of $C_2H_4^+$ and $O_2^{\bullet+}$, and allowing for the 35% channel to $C_2H_4^+$ from the $O_2^{\bullet+}$/propane reaction plus the 5% channel of the $O_2^{\bullet+}$/butane reaction. Finally methane concentrations are determined by the ratio of *m/z* 47 ($CH_2OOH^+$) with $O_2^{\bullet+}$, which incurs substantially more uncertainty due to the very slow reaction rate.

Subtractions are made for isotope overlap from large common ions; e.g., the carbon 13 peak of $C_3H_7^+$ at *m/z* 44 which overlaps with $C_3H_8^+$.

Branched hydrocarbons can also be added to the GeoVOC method by monitoring the $NO^+$ reagent ion and the hydride abstraction product ion for each branched hydrocarbon as $NO^+$ is known not to react at an appreciable rate with the *n*-alkanes [14]. Isobutane, isopentane and isohexane reactions with $NO^+$ from the literature are given in reactions (5)–(7) [15,30,42]. The effects of each branched hydrocarbon reacting with $O_2^{\bullet+}$ must then be subtracted when attempting to determine the respective linear hydrocarbon concentration. Literature values of the reaction rate coefficient for some reactions of $O_2^{\bullet+}$ reacting with branched hydrocarbons are known [10], where the values are unknown, calibration to a known standard is required.

$$NO^+ + i\text{-}C_4H_{10} \rightarrow C_4H_9^+ + NOH \quad (1.00)$$
$$k = 0.9 \times 10^{-9}\,cm^3\,molecule^{-1}\,s^{-1}$$
$$\Delta H^\circ = -39\,kJ\,mol^{-1} \quad (5)$$

$$NO^+ + i\text{-}C_5H_{12} \rightarrow C_5H_{11}^+ + NOH \quad (1.00)$$
$$k = 1.4 \times 10^{-9}\,cm^3\,molecule^{-1}\,s^{-1}$$
$$\Delta H^\circ = -36\,kJ\,mol^{-1} \quad (6)$$

$$NO^+ + i\text{-}C_6H_{14} \rightarrow C_6H_{13}^+ + NOH \quad (1.00)$$
$$k = 1.2 \times 10^{-9}\,cm^3\,molecule^{-1}\,s^{-1} \quad (7)$$

### 4.2. Comparison to standards

Three standard mixtures in nitrogen have been used for validating the GeoVOC method in both dry and wet environments. These are a 15 ppmv standard mixture in nitrogen supplied by Scott Specialty Gases, an 'Iso' standard mixture of isobutane, isopentanes and isohexanes also supplied by Scott Specialty Gases and a "50 ppmv" mixture of $CH_4$, $C_2H_6$, $C_3H_8$ and *n*-$C_4H_{10}$ supplied by BOC. The Scott Specialty gas standards have a stated uncertainty of ±10% and the BOC mixture does not list their uncertainty. Table 4 gives the expected concentration (from supplier) and the empirical concentration as determined by the GeoVOC method on a standard Voice100 instrument using a Nafion dryer system. Fig. 3 then shows the measurement of the 15 ppmv $C_1$–$C_6$ standard with and without the Nafion dryer system.

The concentrations measured by the Voice100 using the GeoVOC method for all standards shown in Table 4 lie within ±30% of the concentration quoted by the suppliers. This error also includes the inherent inaccuracy of the quoted concentration (generally between ±10% and ±20%). The RMS value of the wet samples is greater than that of the dry samples, however it is still small at only 5.9%. The largest deviations from the expected concentrations are found for methane and the branched hydrocarbons. Methane is expected to have the largest uncertainty due to the very slow reaction rate with $O_2^{\bullet+}$. The 'Iso' standard generally reports concentrations lower than the

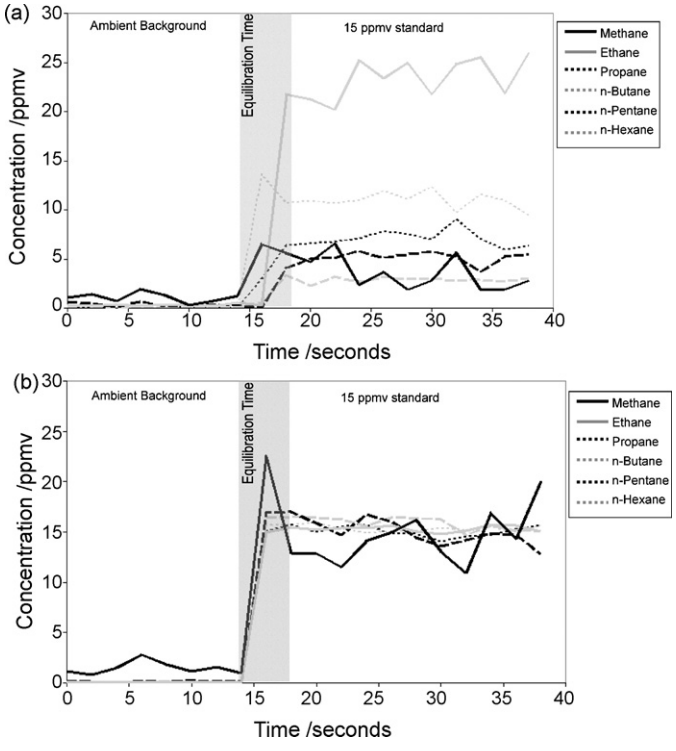


Fig. 3. Example of Nafion drying efficiency in GeoVOC method. Chart (a) shows a wet '15 ppmv' standard mixture of hydrocarbons on a Voice100 *without* an in-line Nafion dryer system; chart (b) shows the same wet '15 PPM' standard on a Voice100 with a Nafion dryer system. In both spectra the ambient air is sampled for the first 15 s to determine a constant background.

Table 4
Reactions of $H_3O^+$ with the given hydrocarbon

| Standard[a] | Hydrocarbon | Quoted conc. (ppmv) | V100 Dry[b] (ppmv) | Error% | V100 Wet[b] (ppmv) | Error% |
|---|---|---|---|---|---|---|
| 15 ppmv | Methane | 15 | 15.3 | +2.6 | 14.1 | −6.2 |
| | Ethane | 15 | 15.8 | +5.1 | 15.2 | +1.4 |
| | Propane | 15 | 14.7 | −1.9 | 14.3 | −4.8 |
| | *n*-Butane | 15 | 14.9 | −0.4 | 14.8 | −1.2 |
| | *n*-Pentane | 15 | 15.6 | +4.3 | 16.0 | +6.5 |
| | *n*-Hexane | 15 | 15.3 | +2.2 | 15.5 | +3.2 |
| 50 ppmv | Methane | 50 | 41.8 | −16.4 | 37.0 | −26.0 |
| | Ethane | 50 | 52.8 | +5.6 | 52.2 | +4.4 |
| | Propane | 50 | 41.6 | −16.8 | 41.6 | −16.8 |
| | *n*-Butane | 50 | 55.1 | +10.2 | 60.7 | +21.4 |
| Iso[c] | Isobutane | 15.6 | 15.4 | −1.1 | 16.5 | +5.8 |
| | Isopentane(s) | 30.6 | 27.3 | −10.9 | 29.5 | −3.6 |
| | Isohexane(s) | 45.4 | 38.8 | −14.5 | 41.2 | −9.4 |
| Mixture[d] | Methane | 7.5 | 9.6 | +28.6 | 8.0 | +6.2 |
| | Ethane | 7.5 | 6.8 | −9.3 | 6.2 | −17.8 |
| | Propane | 7.5 | 9.2 | +22.9 | 8.7 | +16.4 |
| | *n*-Butane | 7.5 | 6.9 | −7.7 | 6.3 | −16.2 |
| | *n*-Pentane | 7.5 | 7.9 | +5.3 | 6.9 | −8.0 |
| | *n*-Hexane | 7.5 | 7.9 | +4.9 | 7.2 | −4.0 |
| | Isobutane | 7.8 | 6.8 | −12.7 | 6.5 | −17.1 |
| | Isopentane(s) | 15.3 | 11.7 | −23.5 | 11.2 | −26.6 |
| | Isohexane(s) | 22.7 | 16.6 | −26.7 | 16.1 | −29.1 |
| RMS | | | 2.0 | | | 5.8 |

[a] Both the '15 ppmv' and 'Iso' (Scott Specialty Gases) have an analytical uncertainty of +/− 10% on the quoted concentration. The '50 ppmv' standard (BOC) does not have a listed analytical uncertainty.
[b] V100 dry and V100 wet refer to measurements made on a Voice100 using dry or wet standards, respectively. Both wet and dry measurements are made using the Nafion drying tube.
[c] The 'Iso' standard contains mixtures of isopentanes and isohexanes which are individually not currently able to be resolved by SIFT-MS.
[d] 'Mixture' refers to a 1:1 mixture of the '15 ppmv' standard and the 'Iso' standard, and therefore is expected to have an analytical uncertainty of at least +/− 20% attributed to the dilution process.

expected value for both the dry and wet samples. This under reporting is possibly attributed to the Nafion tubing interacting with the very slightly polar branched hydrocarbons and affecting the transmitted concentration.

## 5. Conclusions

SIFT-MS using the GeoVOC method is a robust method for the analysis of hydrocarbons from oil and gas seeps across the range of humidities commonly found in soil and water samples. The integration of a Nafion dryer into the Voice100's inlet system allows samples to be dried to a low humidity, which reduces the effect of water secondary chemistry enough for it to be ignored. Because the SIFT-MS technique is very rapid with a throughput of 60 samples per hour, without introducing automated sampling procedures, the SIFT-MS GeoVOC method is a highly cost effective method for oil and gas exploration. Automation would speed up the process even further.

## Acknowledgements

G.J.F. thanks Technology New Zealand for the award of a Ph.D. scholarship. P.F.W thanks the Marsden fund for the award of a postdoctoral fellowship. D.B.M. and V.S.L. thank FRST for the award of postdoctoral fellowships.

## References

[1] V.T. Jones, M.D. Matthews, D.M. Richers, Geochemical Remote Sensing of the Subsurface in Handbook of Exploration Geochemistry, 7, Elsevier, Amsterdam, 1999.
[2] L.S Gournay, J.W. Harrell, C.L. Dennis, Remote sensing of hydrocarbon gas seeps utilizing microwave energy. U.S. Patent No. 4,132,943. U.S. Patent Office, 1979.
[3] V.T. Jones, R.J. Drozd, Amer. Assoc. Petroleum Geol. Bull. 67 (1983) 932.
[4] A. Criado, S. Cardenas, M. Gallega, M. Valcarcel, J. Chromatogr. A 1050 (2004) 111.
[5] P. Spanel, D. Smith, Med. Biol. Eng. Comput. 34 (1996) 409.
[6] C.G. Freeman, M.J. McEwan, Aust. J. Chem. 55 (2002) 491.
[7] D. Smith, P. Spanel, Mass Spectrom. Rev. 24 (2005) 661.
[8] P.F. Wilson, C.G. Freeman, M.J. McEwan, Int. J. Mass. Spectrom. 229 (2003) 1439.
[9] D.B. Milligan, P.F. Wilson, C.G. Freeman, M. Meot-Ner, M.J. McEwan, J. Phys. Chem. A 34 (2002) 9745.
[10] P. Spanel, D. Smith, Int. J. Mass Spectrom. 181 (1998) 1.
[11] D.B. Milligan, D.A. Fairley, C.G. Freeman, M.J. McEwan, Int. J. Mass. Spectrom. 202 (2000) 351.
[12] G.J. Francis, D.B. Milligan. Improvements in or relating to SIFT-MS instruments. N.Z. Patent Number 549242. New Zealand Patent Office, 2006.
[13] E.E. Ferguson, F.C. Fehsenfeld, A.L. Schmeltekopf, Advances in Atomic and Molecular Physics, vol. 5, Academic Press, New York, 1969, p. 1.
[14] V.G. Anicich, J. Phys. Chem. Ref. Data 22 (1993) 1469.
[15] T. Su, W.J. Chesnavich, J. Chem. Phys. 76 (1982) 5183.
[16] D. Lide (Ed.), CRC Handbook of Chemistry and Physics, 86th ed., CRC Press, Boca Raton, 2006.

[17] P.F. Wilson, B.J. Prince, M.J. McEwan, Anal. Chem. 78 (2006) 575.
[18] D.B. Milligan, G.J. Francis, B.J. Prince, M.J. McEwan, Anal. Chem. 79 (2007) 2537.
[19] G.J. Francis, D.B. Milligan, M.J. McEwan, J. Phys. Chem. A 111 (2007) 9670.
[20] W. Janicki, L. Wolska, W. Wardencki, J. Namiesnik, J. Chromato. A. 654 (1993) 279.
[21] D. Mackay, W.Y. Shiu, J. Phys. Chem. Ref. Data 15 (1998) 911.
[22] S.G. Lias, J.E. Bartmess, J.F. Liebman, J.L. Holmes, R.D. Levin, W.G. Mallard, Ion Energetics Data, in: P.J. Linstrom, W.G. Mallard (Eds.), NIST Chemistry WebBook, NIST Standard Reference Database Number 69, National Institute of Standards and Technology, Gaithersburg MD, 2005, p. 20899, http://webbook.nist.gov.
[23] J.M. Van Doren, S.E. Barlow, C.H. DePuy, V.M. Bierbaum, I. Dotan, E.E. Ferguson, J. Phys. Chem. 90 (1986) 2772.
[24] S.E. Barlow, J.M. Van Doren, C.H. DePuy, V.M. Bierbaum, I. Dotan, E.E. Ferguson, N.G. Adams, D. Smith, B.R. Rowe, J.B. Marquette, G. Dupeyrat, M. Durup-Ferguson, J. Chem. Phys. 85 (1986) 3851.
[25] D. Smith, N.G. Adams, J. Chem. Phys. 69 (1978) 308.
[26] S. Matsuoka, Y. Ikazoe, J. Phys. Chem. 92 (1988) 1126.
[27] P. Spanel, D. Smith, J. Chem. Phys. 104 (1996) 1893.
[28] S.T. Arnold, A.A. Viggiano, R.A. Morris, J. Phys. Chem. A. 101 (1997) 9351.
[29] D.B. Milligan, P.F. Wilson, C.G. Freeman, M. Meot-ner, M.J. McEwan, J. Phys. Chem. A 106 (2002) 9745.
[30] S.T. Arnold, A.A. Viggiano, R.A. Morris, J. Phys. Chem. A 102 (1998) 8881.
[31] V.L. Talrose, E.L. Frankevitch, J. Am. Chem. Soc. 80 (1958) 2344.
[32] W.T. Huntress Jr., Astrophys. J. Supp. Ser. 33 (1977) 495.
[33] J.J. DeCorpo, M.V. McDowell, F.E. Saalfeld, J. Phys. Chem. 76 (1972) 1517.
[34] L.W. Sieck, S.K. Searles, J. Chem, Phys. 53 (1970) 2601.
[35] W. Lindinger, D.L. Albritton, M. McFarland, F.C. Fehsenfeld, A.L. Schmeltekopt, E.E. Ferguson, J. Chem. Phys. 62 (1975) 4101.
[36] E.E. Ferguson, Structure, Reactivity and Thermochemistry of Ions, D. Reidel Publ. Co, Boston, 1987.
[37] H. Bohringer, M. Durup-Ferguson, D.W. Fahey, F.C. Fehsenfeld, E.E. Ferguson, J. Chem. Phys. 79 (1983) 4201.
[38] M. Durup-Ferguson, H. Bohringer, D.W. Fahey, F.C. Fehsenfeld, E.E. Ferguson, J. Chem. Phys. 81 (1984) 2657.
[39] H.Y. Afeefy, J.F. Liebman, S.E. Stein, Neutral Thermochemical Data, in: P.J. Linstrom, W.G. Mallard (Eds.), NIST Chemistry WebBook, NIST Standard Reference Database Number 69, National Institute of Standards and Technology, Gaithersburg MD, 2005, p. 20899, http://webbook.nist.gov.
[40] V.G. Anicich, P.F. Wilson, M.J. McEwan, J. Am. Soc. Mass Spectrom. 14 (2003) 900.
[41] P. Spanel, D. Smith, Rapid Commun. Mass Spectrom. 15 (2001) 563.
[42] S.K. Searles, J.L. Franklin, J. Chem. Phys. 52 (1970) 5767.